Phytoplankton growth and consumption by microzooplankton stimulated by turbulent nitrate flux suggest rapid trophic transfer in the oligotrophic Kuroshio

Toru Kobari[1*], Taiga Honma[2], Daisuke Hasegawa[3], Naoki Yoshie[4], Eisuke Tsutsumi[5], Takeshi Matsuno[6], Takeyoshi Nagai[7], Takeru Kanayama[2], Fukutaro Karu[2], Koji Suzuki[8], Takahiro Tanaka[3], Xinyu Guo[4], Gen Kume[1], Ayako Nishina[1] and Hirohiko Nakamura[1]

[1]Aquatic Sciences, Faculty of Fisheries, Kagoshima University
4-50-20 Shimoarata, Kagoshima, Kagoshima 890-0056, Japan
[2]Aquatic Sciences, Graduate School of Fisheries, Kagoshima University
4-50-20 Shimoarata, Kagoshima, Kagoshima 890-0056, Japan
[3]Tohoku National Fisheries Research Institute, Japan Fisheries Research and Education Agency
3-27-5 Shinhama-cho, Shiogama, Miyagi 985-0001, Japan
[4]Center for Marine Environmental Studies, Ehime University
2-5 Bunkyo-cho, Matsuyama, Ehime 790-8577, Japan
[5]Atmosphere and Ocean Research Institute, University of Tokyo
5-1-5 Kashiwanoha, Kashiwa, Chiba 277-8564, Japan
[6]Research Institute for Applied Mechanics, Kyushu University
6-1 Kasuga-koen, Kasuga, Fukuoka 816-8580, Japan
[7]Department of Ocean Sciences, Tokyo University of Marine Science and Technology
4-5-7 Konan Minato-ku, Tokyo 108-8477, Japan
[8]Faculty of Environmental Earth Science, Hokkaido University
North 10 West 5 Kita-ku, Sapporo, Hokkaido 060-0810, Japan

Correspondence to: Toru Kobari (kobari@fish.kagoshima-u.ac.jp)

Abstract. The Kuroshio Current has been thought to be biologically unproductive because of its oligotrophic conditions and low plankton standing stocks. Even though vulnerable life stages of major foraging fishes risk being entrapped by frontal eddies and meanders and encountering low food availability, they have life-cycle strategies that include growing and recruiting around the Kuroshio Current. Here we report that phytoplankton growth and consumption by microzooplankton is stimulated by turbulent nitrate flux amplified by the Kuroshio Current. Oceanographic observations demonstrate that the Kuroshio Current topographically enhances significant turbulent mixing and nitrate influx to the euphotic zone. Graduated nutrient enrichment experiments show that growth rates of phytoplankton and micro-heterotroph communities were stimulated within the range of the turbulent nitrate flux. Results of dilution experiments imply significant microzooplankton grazing on phytoplankton. We propose that these rapid and systematic trophodynamics enhance biological productivity in the Kuroshio.

1 Introduction

The Kuroshio Current is the western boundary current of the North Pacific Subtropical Gyre (Qiu, 2001; Hu et al., 2015). The Kuroshio enters the East China Sea from the east of Taiwan and flows along the continental slope until it passes through the Tokara Strait into the western North Pacific (Fig. 1a). The Kuroshio has been thought to be biologically unproductive because ambient nutrient concentrations and plankton standing stocks in its waters are low (Guo, 1991; Hirota, 1995). In spite of such seemingly unproductive conditions, the Kuroshio in the East China Sea (ECS-Kuroshio) is adjacent to major spawning and nursery grounds of foraging species such as sardines (Watanabe et al., 1996), jack mackerel (Sassa et al., 2008), chub mackerel (Sassa and Tsukamoto, 2010), and common squid (Bower et al., 1999). Indeed, good fishing grounds have been found for various fishes and squid near the Kuroshio, and the catches from those grounds account for more than half of the total catch in Japanese waters (Saito, 2019). It is risky, however, for highly vulnerable early life stages of many foraging species to grow and recruit in the oligotrophic and unproductive waters of the ECS-Kuroshio (hereafter called the “Kuroshio Paradox”: Saito, 2019), even if the warm temperatures of the Kuroshio Current can enhance cellular metabolic processes and thereby stimulate growth. Conventional wisdom is that survival of these early stages is supported by the high plankton productivity on the continental shelf and in the Kuroshio front (Nakata et al., 1995). However, these areas of high productivity are limited in extent and spatiotemporally highly variable because the Kuroshio Current often meanders (Nakata and Hidaka, 2003). Coastal water masses are sometimes entrapped and transported into the Kuroshio and to more pelagic sites (Nakamura et al., 2006; Kobari et al., 2019). Use of waters in the vicinity of the oligotrophic Kuroshio as a nursery and feeding ground would therefore appear to be a risky strategy unless there is a mechanism that enhances biological production in

56 the Kuroshio.

57 There is increasing information about the community structure of phytoplankton and zooplankton in the Kuroshio.
58 Phytoplankton standing stocks in the Kuroshio consist mainly of picoplankton and nanoplankton, and the predominant
59 components are haptophytes, diatoms, and unicellular cyanobacteria like *Prochlorococcus* and *Synechococcus*
60 (Hasegawa et al., 2019; Endo and Suzuki, 2019). Heterotrophic bacteria and calanoid copepods contribute to
61 heterotrophic biomass in the Kuroshio, whereas microzooplankton biomass is relatively small (Kobari et al., 2019).
62 Based on a mass balance model, Kobari et al. (2019) have concluded that mesozooplankton standing stocks in the
63 Kuroshio are supported by micro- and nano-autotrophs and microzooplankton. However, we have little understanding
64 of how biogeochemical processes and trophodynamics support the plankton community in the Kuroshio.

65 In recent years, some mechanisms that supply nutrients to the oligotrophic waters of the Kuroshio have been
66 identified. The Kuroshio “nutrient stream” characterized by an intense core of nutrient flux at subsurface contributes
67 substantially to productivity in the euphotic zone of the Kuroshio in a manner similar to the contribution of the “nutrient
68 stream” along the Gulf Stream (Komatsu and Hiroe, 2019). Turbulence around the Kuroshio appears to be an important
69 mechanism that supplies nutrients via upward movement of deeper waters into the Kuroshio (Nagai et al., 2019).
70 Frontal disturbances also contribute to the supply of nutrients into the euphotic zone of the Kuroshio (Kuroda, 2019).
71 Moreover, the Island Mass Effect produced by the Kuroshio Current as it flows over the bottom topography of the
72 Japanese archipelago induces an upward supply of nutrients (Hasegawa, 2019). These nutrient supplies have been
73 hypothesized to stimulate biological productivity in the Kuroshio. Within the wide path of the Kuroshio, the supply of
74 nutrients by these mechanisms can be particularly efficacious around the Tokara Straits because of the extensive frontal
75 disturbances (Nakamura et al., 2006) and strong turbulence (Tsutsumi et al., 2017; Nagai et al., 2017, 2019) in that area.

Here we report evidence of phytoplankton productivity and subsequent microzooplankton grazing stimulated by turbulence-induced nitrate fluxes in the Kuroshio Current. Oceanographic observations demonstrated a substantial nitrate flux caused by turbulent mixing in the Tokara Strait of the ECS-Kuroshio. Nutrient-amended bottle incubation experiments showed that the growth rates of phytoplankton and micro-heterotrophs, as well as the grazing rates of microzooplankton on phytoplankton, were elevated within the area impacted by this turbulence-induced nitrate flux.

2 Materials and methods

2.1 Onboard observations and experiments

All oceanographic observations and bottle incubations were done in the Kuroshio Current where it passes through the Tokara Strait. Samplings for nitrate concentrations and measurements of turbulent diffusivity were conducted at 14 stations along two transects across the Kuroshio Current (Fig. 1a) during cruises of the T/S *Kagoshima-maru* in November 2015.

The nitrate profiles were measured with a nitrate sensor (Deep SUNA V2) attached to a SBE 9plus conductivity-temperature-depth (CTD) system (Sea Bird Electronics). Turbulent diffusivity was estimated from microstructure measurements made with a microstructure profiler (TurboMAP-L, JFE Advantech Co., Ltd.) and the equations of Osborn (1980). The profiler was deployed immediately after each CTD cast at the same station. The nitrate sensor was calibrated with measured nitrate concentrations (Fig. S1). Because the precision of the nitrate sensor in this study was 0.37 mmol m^{-3} (estimated by Hasegawa et al., 2019), if we had calculated the vertical nitrate gradient from the raw data, the noise level would have been too high to resolve the normal background nitrate stratification of O (10^{-1} mmol m^{-4}). We therefore needed to average the sensor data vertically to reduce the level of noise. The bin-averaged

vertical gradient of the sensor data can be written as follows:

$$\frac{\partial \overline{Cs}}{\partial z} \sim \frac{\overline{Cr}_i - \overline{Cr}_{i-1}}{\Delta z} \pm P\sqrt{\frac{2\bar{w}}{\Delta z^3 f}} \quad (1)$$

where Cs is the nitrate concentration reported by the sensor, Cr is the real concentration, $\bar{w}$ is the average vertical deployment speed of the sensor, f is the sampling frequency, and Δz is the average bin size. In this study f = 1 Hz and $\bar{w}$ = 0.5 m s^{-1}. The second term on the right side of Eq. (1) indicates the expected precision of the bin-averaged vertical gradient of nitrate (see the detailed discussions in Hasegawa et al., 2019). In this study, we set Δz = 10 m to resolve the likely vertical gradient with an expected imprecision of O (10^{-2} mmol m^{-4}).

A total of sixteen nitrate and turbulent diffusivity profiles were averaged at the stations that were studied during the KG1515 cruise of the T/S *Kagoshima-maru* across the Kuroshio path. The profiles of the gradients of the averaged nitrate concentrations and averaged turbulent diffusivity were then multiplied at each depth to calculate the average turbulent nitrate fluxes. Both parameters were binned and averaged within 10-meter intervals. The vertical gradient of the averaged nitrate profile (C_{NO3}) and the averaged vertical diffusivity (K_z) were then multiplied at each depth (z) to estimate the area-averaged vertical turbulent nitrate flux (F_{NO3}) as follows:

$$F_{NO3} = -K_Z \times \partial C_{NO3} / \partial z \quad (2)$$

In recent years, there has been a lively discussion about the importance of the diapycnal advective flux associated with the diffusive flux (e.g., Du et al., 2017). However, in the present study, we assumed that the important nutrient flux was the flux across the base of the euphotic zone, not the flux through the pycnocline, which can be broken down by turbulent mixing. In addition, because our study area included frontal regions, unlike the South China Sea where the

113 Kuroshio flows over seamounts, density fluctuations could have been caused not only by turbulent mixing but also by
114 advection and the movement of fronts. Accordingly, we focused our analysis on the vertical turbulent nutrient flux using
115 Cartesian coordinates rather than on the diapycnal flux using isopycnal coordinates.

116 We performed two different types of bottle incubations. For phytoplankton and micro-heterotrophs, growth rates in
117 response to in situ nitrate fluxes induced by turbulent mixing were estimated using bottle incubations with nutrient
118 gradients (EXP_a) at eight stations in both November 2016 and November 2017. To estimate microzooplankton grazing
119 rates on phytoplankton, dilution experiments (EXP_b) following the methodology of Landry and Hasset (1982) were
120 performed at eight stations in November 2017 (Fig. 1b, Table 1).

121 **2.2 Experimental setup**

122 Seawater samples for all experiments were obtained using 2.5-L Niskin-X bottles attached to a CTD profiler and
123 carousel multisampling system (CTD-CMS: SBE 9plus, Sea Bird Electronics). The samples were transferred by gravity
124 filtration using a silicon tube with a nylon filter (0.1-mm mesh opening) into the incubation bottles for EXP_a and EXP_b.

125 The EXP_a experiment was performed using duplicate 2.3-L polycarbonate bottles without added nutrients and with
126 a mixture of nitrate ($NaNO_3$) and phosphate (KH_2PO_4) in an atomic N:P ratio of 15:1. The nitrate concentrations were
127 either 0 (control), 0.05, 0.15, 0.5, 0.75, 1.5, or 5 μmol L^{-1}. If the turbulent nitrate influx at the subsurface chlorophyll
128 maximum observed in the Tokara Strait (*O*: 0.788 mmol m^{-2} d^{-1}, see Results) were continued for 5.3 days while the
129 Kuroshio Current (0.33 m s^{-1}, Zhu et al., 2017) passed through the Tokara Strait (150 km), the phytoplankton in a layer
130 10 m thick could have consumed nitrate equivalent to a nitrate enrichment of 0.41 μmol L^{-1}.

131 The EXP_b experiment was conducted using triplicate 1.2-L polycarbonate bottles with microzooplankton as

grazers and involved dilutions of the microzooplankton standing stocks in the original water samples so that the concentrations of microzooplankton equaled 1, 0.6, 0.3, or 0.1 times the concentration in the undiluted water. These treatment bottles were enriched with 3 μmol L^{-1} nitrate ($NaNO_3$) and 0.2 μmol L^{-1} phosphate (KH_2PO_4) to promote phytoplankton growth. In addition, to evaluate nutrient limitation of phytoplankton growth, extra triplicate undiluted bottles were incubated without nutrient amendments.

All incubation bottles were soaked in 10% HCl and rinsed with surface seawater at each station before use (Landry et al., 1995). All experimental bottles were incubated for 72 h for EXP_a and 24 h for EXP_b in a water bath with running surface seawater for temperature control and were covered by nylon mesh screening (i.e., screening with 5-mm openings) to reduce irradiance to 75% of the surface irradiance. Phytoplankton growth in the incubation bottles might have been an overestimate of in situ growth because subsurface irradiance was lower than the irradiance in the incubation bottles.

2.3 Sample analysis

Chlorophyll *a* concentrations were determined at the beginning and end of the EXP_a and EXP_b incubations. Subsamples of 500–1000 mL were filtered through a nylon mesh (11-μm mesh opening: Millipore NY1104700) and a glass-fiber filter (2-μm: Whatman GM/F; 0.7-μm: Whatman GF/F) for EXP_a and through a glass-fiber filter (GF/F) for EXP_b at a pressure less than 20 kPa. Photosynthetic pigments were extracted overnight in *N,N*-dimethylformamide at –20 °C in the dark, and the chlorophyll *a* concentrations were determined with a fluorometer (Turner Designs 10AU or TD700). Size fractions were defined as Pico for chlorophyll in phytoplankton smaller than 2 μm, Nano for chlorophyll in phytoplankton between 2 and 11 μm in size, and Micro for chlorophyll in phytoplankton larger than 11 μm.

151 Micro-sized heterotrophs in the incubation bottles at the beginning of EXP_a and EXP_b were examined. Subsamples
152 of 500 mL were collected and fixed with 3% acid Lugol's solution. We identified and counted three taxonomic groups
153 of the micro-heterotroph community (naked ciliates, tintinnids and copepod nauplii) with an inverted microscope (Leica
154 Leitz DMRD). Some marine planktonic ciliates and flagellates are known to be mixotrophs (Gaines and Elbrächter,
155 1987), but we assumed naked ciliates and tintinnids to be heterotrophic in the present study. The sizes of cells or of
156 individuals were measured, the biovolume was computed based on geometric shape, and the carbon content was
157 estimated using conversion equations (Put and Stoecker, 1989; Verity and Langdon, 1984; Parsons et al., 1984).

158 **2.4 Rate calculations**

159 Apparent growth rates (g: d^{-1}) in the incubation bottles of EXP_a and EXP_b were calculated from size-fractionated
160 chlorophyll *a* concentrations (μg L^{-1}) or standing stocks (μg C L^{-1}) of micro-heterotroph groups identified at the
161 beginning (C_o) and end (C_t) of the incubations period (t: days):

162 $$g = [\ln(C_t) - \ln(C_o)]/t \quad (3)$$

163 C_t in the incubation bottles of EXP_b can be calculated using the following equation (Landry et al., 1995):

164 $$C_t = C_o \times \exp[(g_{max} - m) \times t] \quad (4)$$

165 where g_{max} and m are the maximum growth rate of size-fractionated phytoplankton (d^{-1}) and their mortality rate by
166 microzooplankton grazing (d^{-1}), respectively. The maximum growth rate (g_{max}) and mortality rate were determined with
167 a linear regression of the apparent growth rate (g) against dilution factor (X):

168 $g = g_{max} - mX$ (5)

169 where m is the mortality rate in the undiluted water (X = 1). All parameters derived from EXP_a and EXP_b are listed in

170 Table 2 and Table 3.

171 **2.5 Data analysis**

172 To quantify the sensitivity of phytoplankton growth rates to nutrient supply rates, we calculated the slopes of linear

173 regressions of growth rates for the size-fractionated chlorophyll *a* concentrations versus the logarithms of the enriched

174 nitrate concentrations. We then computed the Pearson correlation coefficient of these slopes to nitrate + nitrite and

175 phosphate concentrations and microzooplankton biomass at the beginning of each incubation. A one-way analysis of

176 variance (ANOVA) with a post-hoc Tukey honestly significant difference test was used to compare maximum growth

177 rates, mortality rates, and net growth rates among the three size fractions.

178 **3 Results**

179 **3.1 Oceanographic observations**

180 Turbulent diffusivity and nitrate concentrations were measured in order to estimate the vertical turbulent nitrate flux

181 along the transects across the Kuroshio Current in the Tokara Strait, where a shallow ridge lies in the path of the

182 Kuroshio. We obtained 16 pairs of vertical profiles of turbulent diffusivity and nitrate concentrations and estimated the

183 averages and 95% confidence intervals of the vertical profiles. The averaged chlorophyll-*a* profile (Fig. 2a), which was

184 recorded with a light-emitting diode fluorometer on a TurboMAP-L profiler, revealed a subsurface chlorophyll

185 maximum (SCM) at 60 m, which was almost coincident with a sharp increase in the nitrate concentration (i.e., the top

of the nitracline). Vertical diffusivity of *O* (10^{-4} m^2 s^{-1}, Fig. 2b) was higher at 70 m than at depths of 80–130 m. Just below the SCM peak, relatively high nitrate concentrations and vertical diffusivity induced vertical turbulent nitrate fluxes of *O* (1 mmol m^{-2} d^{-1}, Fig. 2c).

3.2 Gradient enrichment experiments (EXP_a)

To evaluate how the turbulent nitrate fluxes measured in the Tokara Strait increased the standing stocks of phytoplankton and micro-heterotrophs in the Kuroshio, we conducted bottle incubations of the phytoplankton and micro-heterotroph communities enriched with different nutrient concentrations (EXP_a). The total chlorophyll *a* concentrations at the beginning of EXP_a averaged among the duplicate samples ranged from 0.15 to 0.52 μg L^{-1} (Table 1). The pico-fractions and nano-fractions accounted for more than 80% of the total chlorophyll *a* (Fig. 3a). All size-fractionated chlorophyll *a* declined or changed little toward the end of the incubations at nitrate enrichments <0.15 μmol L^{-1}, but they increased at enrichments >0.5 μmol L^{-1}.

At the beginning of the incubations, micro-heterotroph standing stocks averaged among the duplicate samples ranged from 0.12 to 0.79 μg C L^{-1} (Table 1). Naked ciliates accounted for 51–96% of the micro-heterotrophic biomass in terms of carbon at the beginning of the incubations. Copepod nauplii were the second greatest contributor to the micro-heterotroph biomass because of their low abundance but large individual body mass; tintinnid ciliates were a minor component of the micro-heterotroph biomass. The standing stocks of all taxonomic groups in the micro-heterotroph category increased with increasing nitrate enrichment (Fig. 3b), but the patterns of increase in response to nutrient enrichment were less clear than was the case for the size-fractionated chlorophyll *a* concentrations.

Based on the changes of the standing stocks between the beginning and end of the incubations, we investigated the

205 growth rates of the chlorophyll and micro-heterotrophs. The growth rates of all size-fractionated chlorophyll increased
206 at higher concentrations of added nitrate (Fig. 4a). Growth rates were negative or close to zero for all size-fractions at
207 nitrate enrichments <0.15 μmol L^{-1}. However, the growth rates of the pico- and micro-sized chlorophyll were positive
208 at nitrate enrichments >0.5 μmol L^{-1}, which were nearly equivalent to the concentrations associated with the turbulent
209 nitrate fluxes observed in the Tokara Strait (see section 2.2). Because micro-heterotroph growth rates varied among
210 stations, the response of micro-heterotroph growth to the nutrient enrichments was ambiguous (Fig. 4b). Growth rates
211 were positive for copepod nauplii at all nitrate enrichments and were higher for both naked and tintinnid ciliates at
212 higher nitrate enrichments. Thus, the standing stocks of phytoplankton and micro-heterotrophs were likely increased by
213 additions of nitrate within the range of fluxes measured in the Tokara Strait.

214 The slope of a linear regression of the growth rates of the size-fractionated chlorophyll and the logarithms of the
215 nitrate enrichments for each incubation provided a metric of the sensitivity of phytoplankton growth rates to nutrient
216 supplies. The steeper slopes at some stations in the upstream Kuroshio in the Tokara Strait compared to the slopes at
217 other stations (Fig. S2) suggested that the apparent phytoplankton growth rates varied with nutrient concentrations or
218 predatory impacts at the beginning of the incubations. To determine whether growth rates of the size-fractionated
219 chlorophyll might have varied with initial nutrient concentrations (bottom-up control) or predator biomasses (top-down
220 control) at the beginning of the experiments, we compared the slopes to the nitrate + nitrite concentrations (Fig. 5a),
221 phosphate concentrations (Fig. 5b), and micro-heterotroph biomasses (Fig. 5c) in the ambient seawater without
222 enrichment. No significant correlation was found between the micro-heterotrophic biomass and the rate of change of
223 any size-fractionated chlorophyll. In contrast, the fact that there was a negative correlation between the slopes for all
224 size fractions and the nitrate + nitrite or phosphate concentrations indicated that the stimulation of the phytoplankton

225 growth rates by nutrients was greater for all chlorophyll size fractions under more oligotrophic conditions. Thus, the
226 variations of phytoplankton growth rates were likely associated with nutrient concentrations at the beginning of the
227 incubations.

228 **3.3 Dilution experiments (EXP_b)**

229 To evaluate how much each size-fractionated phytoplankton population was removed by microzooplankton grazing, we
230 conducted dilution experiments concurrently with the gradient enrichment experiments. The maximum growth rates
231 (i.e., the intercepts of the regressions corresponding to $X = 0$ in Eq. (5)) were relatively high for the nano-chlorophyll
232 (Fig. 6a), but the differences were insignificant among the three size fractions (ANOVA, $p > 0.05$). These results
233 indicated that the growth potential in the absence of microzooplankton grazing was similar for the nano-sized
234 chlorophyll compared with the pico- and micro-fractions. In contrast, the slopes of the regressions are the mortality
235 rates due to microzooplankton grazing, and the fact that they were significantly higher for the nano-chlorophyll versus
236 the pico- and micro-chlorophyll (ANOVA + Tukey, $p < 0.05$) indicated that the microzooplankton preferentially grazed
237 on the nano-chlorophyll.

238 To evaluate the impact of microzooplankton grazing on phytoplankton growth, we compared three different net
239 growth rates: the observed net growth rates without enrichment (g_o), the net growth rates with enrichment (g_{en}) in the
240 undiluted bottles, and the net growth rates (g_{en}') estimated by subtracting the mortality rate (m) from the maximum
241 growth rates (g_{max}). For all size-fractionated chlorophyll, the fact that g_o was lower than g_{en} (Fig. 7) indicated that net
242 growth rates were limited by nutrients. The values of g_{en} and g_{en}' were comparable, i.e., there was no significant
243 difference between the two (Welch's t-test). These results implied that the g_{en} of all size-fractionated chlorophyll could

244 balance microzooplankton grazing mortality by growing at the maximum rate. In the case of the nano-chlorophyll, the
245 net growth rates were a bit low because the mortality rates due to microzooplankton grazing exceeded the maximum
246 growth rates.

247 **4 Discussion**

248 The Kuroshio Current impinges on numerous shallow ridges with small islands and seamounts in the Tokara Strait.
249 Several studies have pointed out that those steep topographic features stir and modify the water column through
250 upwelling (Hasegawa et al., 2004, 2008) and turbulent mixing (Tsutsumi et al., 2017; Nagai et al., 2017). Compared
251 with the turbulent nitrate fluxes reported in previous studies, the fluxes observed in the Tokara Strait were one order of
252 magnitude higher than those reported in the Kuroshio Extension front (Kaneko et al., 2012, 2013; Nagai et al., 2017),
253 much greater than those at other oceanic sites, and equivalent to those at coastal sites (Cyr et al., 2015). The turbulent
254 nitrate flux in the downstream Kuroshio Current near the Tokara Strait is similar in magnitude to our estimates (Nagai et
255 al., 2019). Because the Kuroshio Current runs steadily through the Tokara Strait, this nutrient supply induced by
256 turbulent diffusivity is considered to be one of the mechanisms that enhance phytoplankton productivity, even under
257 oligotrophic conditions in the Kuroshio Current.

258 Despite the large turbulent nitrate flux (O: 1 mmol m^{-2} d^{-1}), the chlorophyll *a* concentrations in the area of the
259 Tokara Strait impacted by the Kuroshio Current were as low as the values reported from nearby areas of the Kuroshio
260 (Kobari et al., 2018, 2019) and oceanic sites in the North Pacific Ocean (Calbet and Landry, 2004). Based on the
261 gradient enrichment experiments, standing stocks and the growth rates of all size-fractionated phytoplankton increased
262 at nitrate enrichments above 0.5 μmol L^{-1}, which were equivalent to the concentrations produced by the observed

turbulent nitrate flux. These results suggest that phytoplankton standing stocks and growth rates are stimulated by the magnitude of the observed turbulent nitrate flux.

In global comparisons, microzooplankton grazing has a significant impact on phytoplankton, particularly at oceanic sites (Calbet and Landry, 2004). Microzooplankton standing stocks in the Kuroshio Current as it passes through the Tokara Strait are lower than those on the continental shelf of the ECS (Chen et al., 2003) and might be removed by mesozooplankton predation (Kobari et al., 2019). The low microzooplankton standing stocks in the Kuroshio Current imply low microzooplankton grazing on phytoplankton. However, the dilution experiments demonstrated that phytoplankton mortality by microzooplankton grazing was high and equivalent to 41–122% of the maximum growth rates of the phytoplankton, based on the ratio of the mortality rate to the maximum growth rates of total chlorophyll *a* (Table 2). Indeed, phytoplankton could likely balance microzooplankton grazing mortality by growing at maximum rates, particularly in the case of the nano-phytoplankton (Fig. 7). These results from concurrently conducted experiments suggested that phytoplankton standing stocks are stimulated by turbulent nitrate fluxes and are then quickly removed by microzooplankton grazing, particularly in the case of nanophytoplankton. Taking into account the size range of prey for ciliates (Pierce and Turner, 1992) and copepod nauplii (Uye and Kasahara, 1983), microzooplankton grazing could be a major reason why phytoplankton do not attain high growth rates and standing stocks, even when their growth potential is high and they are sensitive to nutrient enrichments. The rapid transfer of the elevated phytoplankton production to microzooplankton might thus be a possible explanation for the low chlorophyll concentrations, even when there are large turbulent nitrate fluxes in the Kuroshio Current.

The standing stocks and growth rates of all micro-heterotrophs were relatively high in the higher nitrate enrichments, but the patterns of increase were less clear than in the case of the phytoplankton. This difference was

283 probably due to the large variations in the micro-heterotroph standing stocks among stations (Table 1) and slower
284 growth than phytoplankton. Indeed, the lack of clarity of this pattern was remarkable for the copepod nauplii because of
285 their relatively slow growth rates, lower abundance in the bottles, and larger individual body masses. In contrast,
286 “intra-guild” predation within micro-heterotroph communities might be another explanation for the ambiguous pattern
287 of their standing stocks and growth rates. The growth rates of copepod nauplii were always higher than those of naked
288 ciliates, especially when there was no or little nitrate supplied. The ratio of mean equivalent spherical diameter of body
289 mass for copepod nauplii (88 μm) and naked ciliates (16 μm) was estimated to be 5:1, which is much different from a
290 typical predator–prey mass ratio (i.e., 18:1, Hansen et al., 1994). Thus, it is unlikely that intraguild predation of copepod
291 nauplii on naked ciliates would happen in the bottles. More importantly to the ambiguous pattern of the growth of the
292 micro-heterotrophs, the results from the concurrently conducted experiments implied that phytoplankton productivity
293 was stimulated by the turbulent nitrate flux and the phytoplankton rapidly grazed by microzooplankton, but standing
294 stocks and growth rates of micro-heterotrophs were not elevated during three days in the Kuroshio Current. An increase
295 of micro-heterotroph standing stocks and their trophic transfer to mesozooplankton might have been apparent further
296 downstream in the Kuroshio Current.

297 There is increasing evidence that turbulence-induced nutrient fluxes promote phytoplankton growth in the open
298 ocean (Kaneko et al., 2013; Nagai et al., 2017, 2019). However, there is no experimental documentation for a response
299 of the phytoplankton community to this nutrient supply or of subsequent trophic transfer in a planktonic food web. In
300 the tropical and subtropical oceans, microzooplankton grazing has been thought to be a major source of phytoplankton
301 mortality and has been shown to account for more than 75% of phytoplankton daily growth (Calbet and Landry, 2004).
302 Furthermore, strong trophic linkages are well known between microbes and metazoans through microzooplankton

(Calbet and Landry, 1999; Calbet et al., 2001; Calbet and Saiz, 2005; Kobari et al., 2010). Our study has provided the first experimental evidence that phytoplankton standing stocks and growth rates are stimulated by turbulent nutrient fluxes and rapidly grazed by microzooplankton. These results imply that biological productivity may be underestimated because of the apparently low nutrient concentrations and low phytoplankton biomass in the Kuroshio. Because of the strong turbulence amplified by the Kuroshio Current, phytoplankton productivity stimulated by nutrient fluxes and rapid trophic transfer to microzooplankton are likely to happen in the Tokara Strait and downstream. We therefore propose that undocumented biological productivity in the Kuroshio is sustained by these rapid and systematic trophodynamics. Such undocumented biological production, elevated by the rapid and systematic trophodynamics, may provide a good supply of food for the vulnerable stages of foraging fishes around the Kuroshio and thus explain part of the Kuroshio Paradox.

Data Availability Statement:

All relevant data are shown in the paper as tables and figure.

Author Contributions

T. Kobari, DH and NY conceived and designed the oceanographic observations and experiments. DH, HN, AN, ET, TM, TN performed the oceanographic observations and turbulence measurements. T. Kobari, TH, T. Kanayama and FK performed the onboard experiments. T. Kobari, TH, T. Kanayama, FK, NY, KS analyzed the samples and data of the onboard experiments. DH and TT analyzed the data of oceanographic observations and turbulence measurements. T. Kobari, GK, HN and XG organized the research cruises.

Competing interests:

The authors declare no competing or conflict interests.

Acknowledgements

We thank the captains and crew of the T/S *Kagoshima-maru* for their help in oceanographic observations and sample collections.

Financial support:

This study has been supported by grants from the Japan Society for the Promotion of Science (17K00522, 18H04920, 4702), Ministry of Education, Culture, Sports, Science and Technology in Japan (The Study of Kuroshio Ecosystem Dynamics for Sustainable Fisheries).

References

Bower, J.R., Nakamura, Y., Mori, K., Yamamoto, J., Isoda, Y., Sakurai, Y.: Distribution of *Todarodes pacificus* (Cephalopoda: Ommastrephidae) paralarvae near the Kuroshio off southern Kyushu, Japan, Mar. Biol., 135, 99–106, 1999.

Calbet, A., Landry, M. R.: Mesozooplankton influences on the microbial food web: Direct and indirect trophic interactions in the oligotrophic open-ocean, Limnol. Oceanogr., 44, 1370–1380, 1999.

Calbet, A., Landry, M. R.: Nunnery S. Bacteria-flagellate interactions in the microbial food web of the oligotrophic subtropical North Pacific, Aquat. Microb. Ecol., 23, 283–292, 2001.

Calbet, A., Landry, M. R.: Phytoplankton growth, microzooplankton grazing, and carbon cycling in marine systems. Limnol. Oceanogr., 49, 51–57, 2004.

Calbet, A., Saiz, E.: The ciliate-copepod link in marine ecosystems, Aquat. Microb. Ecol., 38, 157–167, 2005.

347 Chen, C. C., Shiah, F.K., Gong, G. C., Chiang, K. P.: Planktonic community respiration in the East China Sea:
348 importance of microbial consumption of organic carbon. Deep-Sea Res. II, 50, 1311–1325, 2003.
349 Cyr, F., Bourgault, D., Galbraith, P. S.: Gosselin M. Turbulent nitrate fluxes in the Lower St. Lawrence Estuary, Canada.
350 J. Geophys. Res., 120, 2308–2330, 2015.
351 Du, C., Liu, Z., Kao, S-J., Dai, M.: Diapycnal fluxes of nutrients in an oligotrophic oceanic regime: the South China
352 Sea. Geophys. Res. Lett., 44, 11510-11518, 2017.
353 Endo, H., Suzuki, K.: Spatial variations in community structure of haptophytes across the Kuroshio front in the Tokara
354 Strait, in: Kuroshio Current, Physical, Biogeochemical and Ecosystem Dynamics, edited by: Nagai, T., Saito,
355 H., Suzuki, K., Takahashi, M., Geophysical Monograph 243, John Wiley & Sons, Hoboken, 207–221, 2019.
356 Gaines, G., Elbrächter. M.: Heterotrophic nutrition, in The biology of dinoflagellates, edited by: Taylor, F. J. R.,
357 Blackwell, Oxford, 224–268, 1987.
358 Guo, Y. J.: The Kuroshio, Part II. Primary production and phytoplankton, Oceanogr. Mar. Bio. Ann. Rev., 29, 155–189,
359 1991.
360 Hansen, B., Bjørnsen, P. K., Hansen, P. J.: The size ratio between planktonic predators and their prey, Limnol.
361 Oceanogr., 39, 395–403, 1994.
362 Hasegawa, D., Island Mass Effect, in: Kuroshio Current, Physical, Biogeochemical and Ecosystem Dynamics, edited
363 by: Nagai, T., Saito, H., Suzuki, K., Takahashi, M., Geophysical Monograph 243, John Wiley & Sons,
364 Hoboken, 163–174, 2019.
365 Hasegawa, D., Tanaka, T., Matsuno, T., Senjyu, T., Tsutsumi, E., Nakamura, H., Nishina, A., Kobari, T., Yoshie, N., Guo,
366 X., Nagai, T., Okunishi, T., Yasuda, I.: Measuring the vertical turbulent nitrate flux using sensors, Bull. Coast.

Oceanogr., 57, 59–64, 2019.

Hasegawa, D., Yamazaki, H., Ishimaru, T., Nagashima, H., Koike, Y.: Apparent phytoplankton bloom due to island mass effect, J. Mar. Syst., 69, 238–246, 2008.

Hasegawa, D., Yamazaki, H., Lueck, R. G., Seuront, L.: How islands stir and fertilize the upper ocean, Geophys. Res. Lett., 31, L16303, 2004.

Hasegawa, T., Kitajima S., Kiyomoto Y.: Phytoplankton distribution in the Kuroshio region of the southern East China Sea in early spring, in: Kuroshio Current, Physical, Biogeochemical and Ecosystem Dynamics, edited by: Nagai, T., Saito, H., Suzuki, K., Takahashi, M., Geophysical Monograph 243, John Wiley & Sons, Hoboken, 191–205, 2019.

Hirota, Y.: The Kuroshio, Part III. Zooplankton, Oceanogr Mar. Bio. Ann. Rev., 33, 151–220, 1995.

Hu, D., Wu, L., Cai, W., Gupta, A. S., Ganachaud, A., Qiu, B., Gordon, A. L., Lin, X., Chen, Z., Hu, S., Wang, G., Wang, Q., Sprintall, J., Qu, T., Kashino, Y., Wang, F., William S. Kessler, W. S.: Pacific western boundary currents and their roles in climate, Nature, 522, 299–308, 2015.

Kaneko, H., Yasuda, I., Komatsu, K., Itoh, S.: Observations of the structure of turbulent mixing across the Kuroshio, Geophys. Res. Lett., 39, L15602, 2012.

Kaneko, H., Yasuda, I., Komatsu, K., Itoh, S.: Observations of vertical turbulent nitrate flux across the Kuroshio, Geophys. Res. Lett., 40, 3123–3127, 2013.

Kobari, T., Kobari, Y., Miyamoto, H., Okazaki, Y., Kume, G., Kondo, R., Habano, A.: Variability in taxonomic composition, standing stock and productivity of the plankton community in the Kuroshio and its neighboring waters, in: Kuroshio Current, Physical, Biogeochemical and Ecosystem Dynamics, edited by: Nagai, T., Saito,

H., Suzuki, K., Takahashi, M., Geophysical Monograph 243, John Wiley & Sons, Hoboken, 223–243, 2019.

Kobari, T., Makihara, W., Kawafuchi, T., Sato, K., Kume, G.: Geographic variability in taxonomic composition, standing stock, and productivity of the mesozooplankton community around the Kuroshio Current in the East China Sea, Fish. Oceanogr., 27, 336–350, 2018.

Kobari, T., Mitsui, K., Ota, T., Ichinomiya, M., Gomi, Y.: Response of heterotrophic bacteria to the spring phytoplankton bloom in the Oyashio region. Deep-Sea Res. II., 57, 1671–1678, 2010.

Komatsu, K., Hiroe, Y.: Structure and impact of the Kuroshio nutrient stream, in: Kuroshio Current, Physical, Biogeochemical and Ecosystem Dynamics, edited by: Nagai, T., Saito, H., Suzuki, K., Takahashi, M., Geophysical Monograph 243, John Wiley & Sons, Hoboken, 85–104, 2019.

Kuroda, H.: The Kuroshio-induced nutrient supply in the shelf and sloe region off the southern coast of Japan, in: Kuroshio Current, Physical, Biogeochemical and Ecosystem Dynamics, edited by: Nagai, T., Saito, H., Suzuki, K., Takahashi, M., Geophysical Monograph 243, John Wiley & Sons, Hoboken, 137–146, 2019.

Landry, M. R., Hasset, R. P.: Estimating the grazing impact of marine micro-zooplankton, Mar. Biol., 67, 283–288, 1982.

Landry, M. R., Kirshtein, J., Constantinou, J.: A refined dilution technique for measuring the community grazing impact of microzooplankton with experimental tests in the central equatorial Pacific, Mar. Ecol. Prog. Ser., 120, 53–63, 1995.

Nagai, T., Clayton, S., Uchiyama, Y.: Multiscale routes to supply nutrients through the Kuroshio nutrient stream, in: Kuroshio Current, Physical, Biogeochemical and Ecosystem Dynamics, edited by: Nagai, T., Saito, H., Suzuki, K., Takahashi, M., Geophysical Monograph 243, John Wiley & Sons, Hoboken, 105–125, 2019.

Nagai, T., Durán, G. S., Otero, D. A., Mori, Y., Yoshie, N., Ohgi, K., Hasegawa, D., Nishina, A., Kobari, T.: How the Kuroshio Current delivers nutrients to sunlit layers on the continental shelves with aid of near-internal waves and turbulence, Geophys. Res. Lett., 46, 10.1029/2019GL082680, 2019.

Nagai, T., Hasegawa, D., Tanaka, T., Nakamura, H., Tsutsumi, E., Inoue, R., Yamashiro, T.: First evidence of coherent bands of strong turbulent layers associated with high-wavenumber internal-wave shear in the upstream Kuroshio, Sci. Rep., 7, 14555, 2017.

Nakamura, H., Yamashiro, T., Nishina, A., Ichikawa, H.: Time frequency variability of Kuroshio meanders in Tokara Strait, Geophys. Res. Lett., 33, L21605, 2006.

Nakata, K., Hidaka, K.: Decadal-scale variability in the Kuroshio marine ecosystem in winter, Fish. Oceanogr., 12, 234–244, 2003.

Nakata, K., Zenitani, H., Inagake, D.: Differences in food availability for Japanese sardine larvae between the frontal region and the waters on the offshore side of Kuroshio, Fish. Oceanogr., 4, 68–79, 1995.

Osborn, T.: Estimates of the local rate of vertical diffusion from dissipation measurements. J. Phys. Oceanogr., 10, 83–89, 1980.

Parsons, T. R., Takahashi, M., Hargrave, B.: Biological oceanographic processes, Pergamon Press, Oxford, 1984.

Pierce, R. W., Turner, J. T.: Ecology of planktonic ciliates in marine food webs, Rev. Aquat. Sci., 6, 139–181, 1992.

Putt, M., Stoecker, D. K.: An experimentally determined carbon:volume ration for marine "oligotrichous" ciliates from estuarine and coastal waters, Limnol. Oceanogr., 34, 1097–1103, 1989.

Qiu, B.: Kuroshio and Oyashio Currents, in: Encyclopedia of Ocean Sciences, edited by: Steele, J. H., Academic Press, New York, 358–369, 2001.

427 Saito, H.: The Kuroshio: its recognition, scientific activities and emerging issues, in: Kuroshio Current, Physical,
428 Biogeochemical and Ecosystem Dynamics, edited by: Nagai, T., Saito, H., Suzuki, K., Takahashi, M.,
429 Geophysical Monograph 243, John Wiley & Sons, Hoboken, 1–11, 2019.
430 Sassa, C., Tsukamoto, Y.: Distribution and growth of *Scomber japonicus* and *S. australasicus* larvae in the southern East
431 China Sea in response to oceanographic conditions, Mar. Ecol. Prog. Ser., 419, 185–199, 2010.
432 Sassa, C., Tsukamoto, Y., Nishiuchi, K., Konishi, Y.: Spawning ground and larval transport processes of jack mackerel
433 *Tranchurus japonicas* in the shelf-break region of the southern East China Sea, Cont. Shelf. Res., 28, 2574–
434 2583, 2008.
435 Tsutsumi, E., Matsuno, T., Lien, R. C., Nakamura, H., Senjyu, T., Guo, X.: Turbulent mixing within the Kuroshio in the
436 Tokara Strait, J. Geophys. Res. Oceans, 122, 10.1002/2017JC013049, 2017.
437 Uye, S. I., Kasahara, S.: Grazing of various developmental stages of *Pseudodiaptomus marinus* (Copepoda: Calanoida)
438 on naturally occurring particles, Bull. Plankton Soc. Japan, 30, 147–158, 1983.
439 Verity, P. G., Langdon, C.: Relationships between lorica volume, carbon, nitrogen and ATP content of tintinnids in
440 Narragansett Bay, J. Plankton Res., 6, 859–868, 1984.
441 Watanabe, Y., Zenitani, H., Kimura, R.: Offshore expansion of spawning of the Japanese sardine, *Sardinops*
442 *melanostictus*, and its implication for egg and larval survival, Can. J. Fish. Aquat. Sci., 53, 55–61, 1996.
443 Zhu, X. H., Nakamura, H., Dong, M., Nishina, A., Yamashiro, T.: Tidal currents and Kuroshio transport variations in the
444 Tokara Strait estimated from ferryboat ADCP data, J. Geophys. Res., 122, 2120–2142, 2017.

Table 1 Location and environmental conditions at the stations in the ECS-Kuroshio where gradient enrichment (EXP_a) and dilution experiments (EXP_b) were conducted. Depth: sampling depth (m) of water samples for each experiment. WT: mean water temperature during the experiments (ºC). $NUTs_o$: nutrients concentrations (µmol L^{-1}) at the beginning of each experiment. CHL_o: Chlorophyll *a* concentration (µgCHL L^{-1}) at the beginning of the experiments. MiZ_o: micro-heterotroph standing stock at the beginning of each experiment (µgC L^{-1}). DL: below the detection limit.

Station	Location		Date	Year	Depth	WT	$NUTs_o$		CHL_o	MiZ_o
	Longitude	Latitude					NO_3+NO_2	PO_4		
EXP_a										
C02	30°11'N	129°41.0'E	13 Nov	2016	68	26.1	DL	0.02	0.34	0.19
C03	29°50'N	129°08.4'E	13 Nov	2016	75	26.2	DL	0.01	0.41	0.27
F01	29°53'N	129°22.4'E	14 Nov	2016	81	25.1	0.21	0.04	0.35	0.15
G01	29°51'N	129°57.2'E	14 Nov	2016	91	26.1	0.26	0.07	0.44	0.12
K02	29°34'N	128°26.3'E	12 Nov	2017	50	25.6	0.18	DL	0.31	0.23
K05	30°06'N	130°11.9'E	14 Nov	2017	105	24.8	0.57	0.02	0.52	0.79
K08	30°24'N	131°23.6'E	15 Nov	2017	115	25.5	1.82	0.12	0.15	0.34
K11	31°24'N	132°29.2'E	16 Nov	2017	90	25.0	0.16	DL	0.27	0.55
EXP_b										
A05a	30°10'N	129°17.5'E	3 Nov	2017	13	25.5	0.10	0.03	0.23	0.12
A05b	30°10'N	129°17.5'E	7 Nov	2017	95	25.5	DL	DL	0.16	0.15
A05c	30°11'N	129°17.2'E	7 Nov	2017	34	25.3	0.02	0.01	0.24	0.05
A06a	30°00'N	129°15.1'E	3 Nov	2017	12	25.4	DL	0.02	0.16	0.13
A06b	30°00'N	129°15.0'E	7 Nov	2017	110	25.7	1.61	0.11	0.14	0.04
A08a	29°19'N	129°09.4'E	6 Nov	2017	76	25.6	DL	0.02	0.29	0.22
A08b	29°26'N	129°12.4'E	6 Nov	2017	71	25.6	0.03	0.01	0.21	0.17
A09a	29°09'N	129°00.0'E	6 Nov	2017	105	25.6	0.11	0.02	0.20	0.15

Table 2 Phytoplankton growth rate (d^{-1}) derived from the gradient enrichment experiments (EXP_a) in the ECS-Kuroshio. Enriched nitrate concentrations (μmol L^{-1}) are shown at the top of each column. A and B: duplicate bottles. Pico: chlorophyll smaller than 2 μm. Nano: chlorophyll between 2 and 11 μm. Micro: chlorophyll larger than 11 μm.

Station	0		0.05		0.15		0.5		0.75		1.5		5	
	A	B	A	B	A	B	A	B	A	B	A	B	A	B
Micro														
C02	-0.108	-0.116	-0.089	-0.082	0.019	-0.073	0.470	0.426	0.422	0.441	0.686	0.798	0.796	0.556
C03	-0.116	-0.118	-0.073	-0.078	-0.004	-0.008	0.453	0.426	0.588	0.706	0.780	0.892	0.862	0.906
F01	0.150	0.159	0.332	0.277	0.282	0.344	0.445	0.495	0.511	0.497	0.490	0.385	0.372	0.467
G01	0.062	0.051	0.135	0.089	0.163	0.108	0.438	0.477	0.795	0.736	0.828	0.969	0.861	0.781
K02	-0.305	-0.282	-0.205	-0.265	-0.113	-0.305	0.264	0.295	0.119	0.097	0.422	0.652	0.831	0.669
K05	-0.147	0.027	0.007	-0.053	0.037	0.084	0.329	0.176	0.263	0.168	0.645	0.716	0.792	0.701
K08	0.348	0.266	0.350	0.315	0.333	0.407	0.361	0.185	0.448	0.416	0.377	0.468	0.403	0.417
K11	-0.062	-0.036	-0.105	-0.092	0.043	-0.081	0.193	0.179	0.514	0.390	0.765	0.730	0.469	0.558
Nano														
C02	-0.479	-0.260	-0.208	-0.409	-0.297	-0.345	-0.050	0.144	0.173	0.151	0.249	0.333	0.330	0.264
C03	-0.275	-0.261	-0.211	-0.257	-0.080	-0.206	0.113	0.031	0.247	0.192	0.363	0.355	0.288	0.256
F01	-0.244	-0.154	-0.286	-0.092	-0.025	0.101	0.182	0.050	0.148	0.039	0.015	0.056	0.104	0.105
G01	-0.304	-0.172	-0.313	-0.189	-0.165	-0.117	-0.063	-0.178	0.100	0.001	0.286	0.325	0.369	0.053
K02	-0.321	-0.149	-0.384	-0.152	0.022	0.035	0.223	0.251	-0.027	-0.135	0.433	0.229	0.559	0.523
K05	-0.389	-0.318	-0.680	-0.546	-0.267	-0.394	-0.484	-0.248	-0.407	-0.458	0.053	-0.034	0.102	0.196
K08	0.353	0.244	0.508	0.472	0.455	0.436	0.406	0.397	0.473	0.369	0.408	0.546	0.380	0.384
K11	-0.138	-0.088	-0.257	-0.243	-0.134	-0.293	0.073	0.026	0.175	0.201	0.296	0.312	0.434	0.501
Pico														
C02	-0.383	-0.188	-0.186	-0.199	-0.119	-0.162	0.188	0.143	0.162	0.241	0.257	0.291	0.377	0.205
C03	-0.202	-0.258	-0.259	-0.282	-0.143	-0.160	0.017	-0.019	0.148	0.191	0.194	0.248	0.230	0.300
F01	-0.071	-0.091	-0.054	-0.032	0.050	0.129	0.205	0.144	0.216	0.141	0.170	0.134	0.031	0.172
G01	0.019	-0.061	0.051	-0.032	0.019	0.008	0.156	0.162	0.323	0.188	0.338	0.308	0.344	0.366
K02	-0.245	-0.253	-0.257	-0.275	-0.243	-0.230	-0.046	0.010	-0.067	-0.101	0.065	-0.030	0.203	0.089
K05	-0.087	0.031	0.014	-0.027	0.103	0.157	0.057	0.261	0.130	0.339	0.316	0.255	0.368	0.404
K08	0.032	0.055	-0.013	0.228	0.262	0.201	0.240	0.069	0.262	0.281	0.177	0.284	0.222	0.327
K11	-0.197	-0.216	-0.194	-0.146	-0.046	-0.071	-0.005	0.033	0.163	0.076	0.236	0.049	0.092	0.179

Table 3 Parameters derived from the dilution experiments (EXP_b) in the ECS-Kuroshio. g_{max}: maximum growth rate (d^{-1}). m: mortality rate by microzooplankton grazing (d^{-1}). g_o: net growth rate measured in the non-enriched and non-diluted bottles (d^{-1}). g_{en}: net growth rate measured in the enriched and non-diluted bottles (d^{-1}). r^2: coefficient of determination defined from the linear regression of the apparent growth rate of total chlorophyll *a* concentrations against dilution factors. *p*: *p*-value. Pico: chlorophyll smaller than 2 µm. Nano: chlorophyll between 2 and 11 µm. Micro: chlorophyll larger than 11 µm. Total: total chlorophyll from pico- to micro.

Station	Pico				Nano				Micro				Total					
	g_{max}	m	g_o	g_{en}	g_{max}	m	g_o	g_{en}	g_{max}	m	g_o	g_{en}	g_{max}	m	g_o	g_{en}	r^2	p
A05a	0.283	0.887	0.415	0.681	1.181	1.345	-0.267	0.181	0.913	0.962	0.059	0.045	1.059	0.619	0.199	0.492	0.757	<0.01
A05b	0.931	1.106	-0.109	0.279	1.354	1.050	-0.505	-0.239	0.477	0.583	-0.030	0.107	1.073	1.051	-0.232	0.113	0.901	<0.01
A05c	0.501	0.647	-0.025	0.190	1.298	1.192	-0.183	-0.066	0.313	0.500	-0.269	0.201	0.828	0.752	-0.074	0.122	0.875	<0.01
A06a	0.179	0.814	0.440	0.646	0.865	1.270	0.247	0.341	0.232	0.597	-0.315	0.339	0.941	0.381	0.347	0.550	0.541	<0.01
A06b	0.648	-0.398	-0.869	-1.020	0.947	0.247	-0.789	-0.629	-0.118	-0.037	-0.038	0.065	-0.052	0.711	-0.735	-0.714	0.750	<0.01
A08a	0.434	0.458	-0.097	0.035	1.448	1.289	-0.072	-0.150	0.401	0.564	-0.537	0.181	0.765	0.775	-0.113	0.009	0.856	<0.01
A08b	0.370	0.846	-0.040	0.509	0.652	1.068	-0.259	0.430	0.553	1.122	-0.620	0.529	0.937	0.471	-0.123	0.488	0.693	<0.01
A09a	0.488	0.417	-0.399	-0.026	0.894	0.734	-0.182	-0.082	0.353	0.022	-0.474	-0.235	0.526	0.640	-0.324	-0.052	0.760	<0.01

Table 4 Parameters derived from relationship of phytoplankton growth rates against logarithmically transformed concentrations of enriched nitrate in the gradient enrichment experiments (EXP_a). Slope: sensitivity of phytoplankton growth rate to logarithmically transformed concentrations of enriched nitrate. Intercept: growth potential at the low nitrate concentration. r^2: coefficient of determination defined from the linear regression of growth rate of size-fractionated chlorophyll *a* concentrations against logarithmically transformed concentrations of enriched nitrate. Pico: chlorophyll smaller than 2 μm. Nano: chlorophyll between 2 and 11 μm. Micro: chlorophyll larger than 11 μm.

Station	Pico			Nano			Micro		
	Slope	Intercept	r^2	Slope	Intercept	r^2	Slope	Intercept	r^2
C02	0.281	0.178	0.848	0.370	0.131	0.831	0.458	0.492	0.846
C03	0.295	0.121	0.922	0.308	0.177	0.830	0.560	0.611	0.914
F01	0.074	0.129	0.317	0.120	0.067	0.420	0.077	0.430	0.368
G01	0.203	0.243	0.866	0.272	0.085	0.688	0.448	0.657	0.817
K02	0.213	-0.014	0.883	0.364	0.233	0.726	0.531	0.353	0.872
K05	0.188	0.251	0.772	0.355	-0.165	0.729	0.419	0.439	0.843
K08	0.070	0.231	0.242	-0.038	0.426	0.213	0.045	0.386	0.162
K11	0.167	0.077	0.750	0.394	0.201	0.943	0.403	0.409	0.744

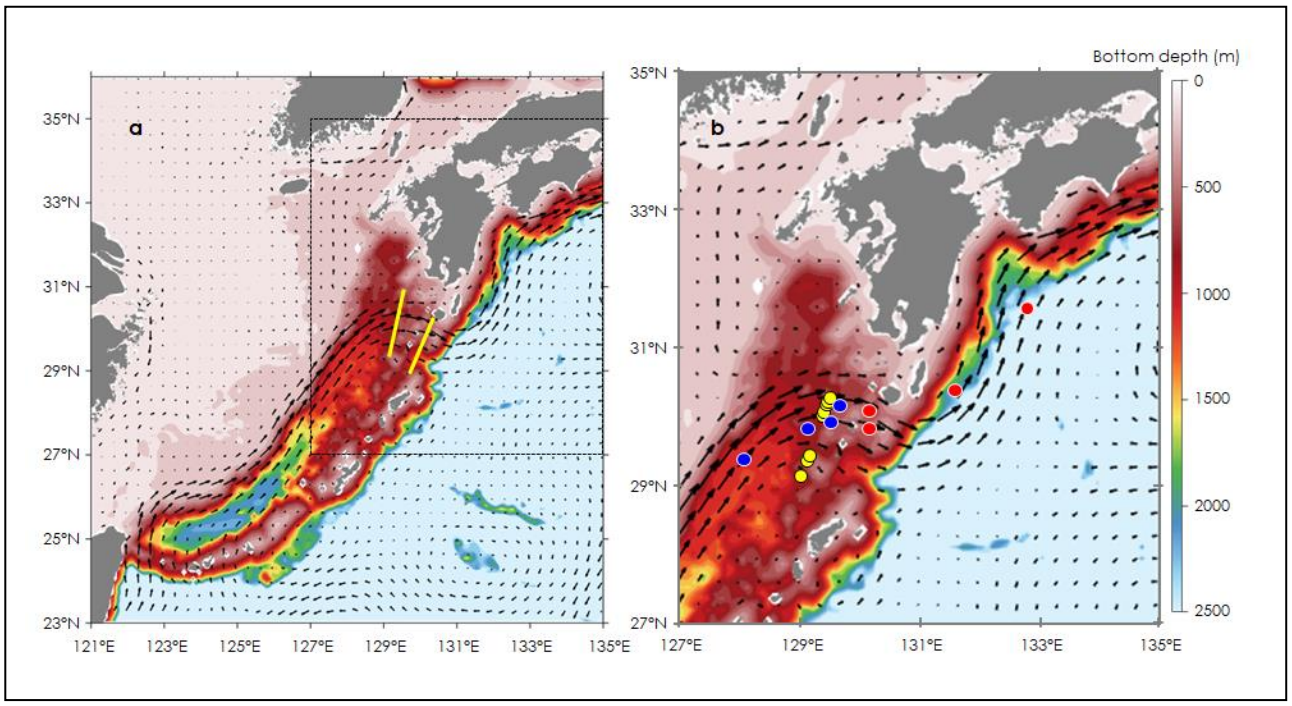

Figure 1 Locations for oceanographic observations and onboard experiments in the Kuroshio Current of the East China Sea (ECS-Kuroshio). **(a)** Oceanographic observations by Deep SUNA V2 and TurboMAP-L (yellow lines). **(b)** Onboard experiments for phytoplankton and microzooplankton growth (EXP_a: red and blue circles) and for microzooplankton grazing (EXP_b: yellow circles). EXP_a was conducted in the upstream (blue circles) and downstream Kuroshio (red circles) in the Tokara Strait. Current directions and velocities (arrows) are shown as monthly means during November 2016. Bottom depth (m) is indicated as colored contours.

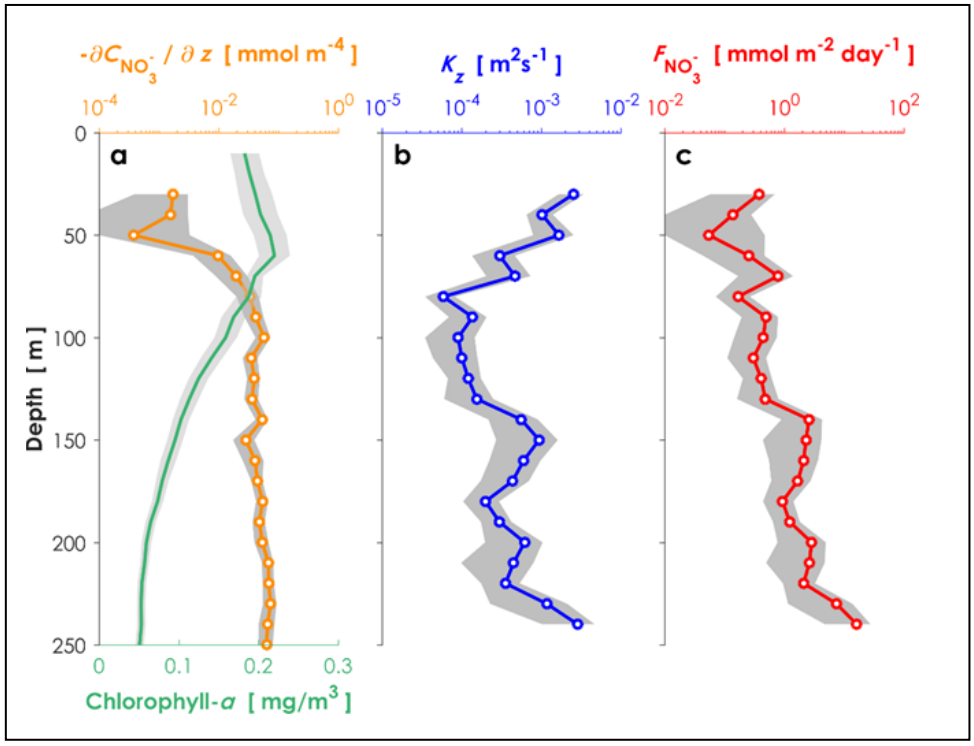

476

477 **Figure 2** Vertical profiles of environmental conditions in the Kuroshio Current. **(a)** Nitrate gradient curve (orange) and
478 chlorophyll *a* concentrations (green) measured with a nitrate sensor (Deep SUNA V2) attached to an SBE-9plus CTD
479 system. **(b)** Turbulent diffusivity measured with a TurboMAP-L (blue). (**c**) Calculated turbulent nitrate fluxes (red) in
480 the ECS-Kuroshio. The shaded areas are the 95 percent confidence intervals obtained by a bootstrap process.

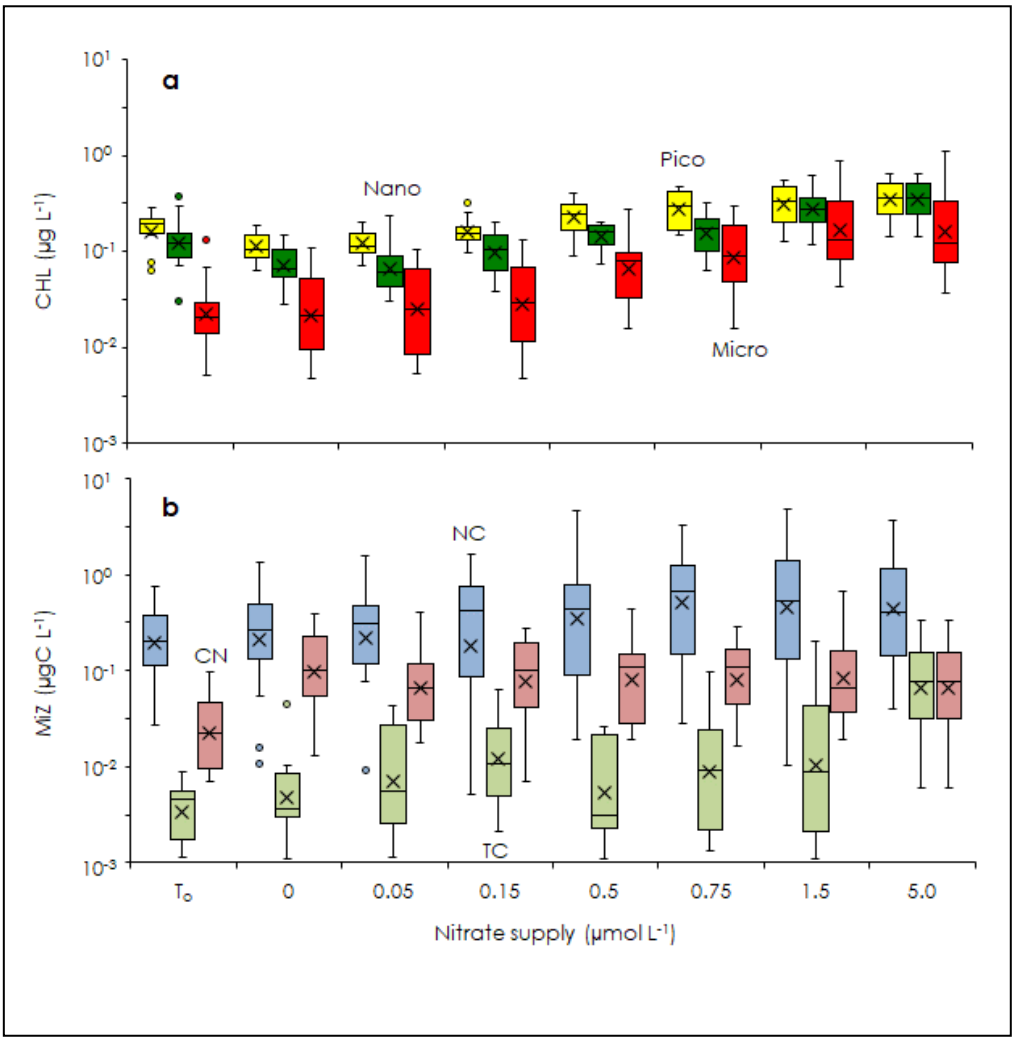

Figure 3 Changes in phytoplankton and micro-sized heterotroph standing stocks during the gradient enrichment experiments (EXP_a). **(a)** Size-fractionated chlorophyll *a* concentrations (CHL). **(b)** Micro-heterotroph standing stocks (MiZ). T_o: at the beginning of the gradient enrichment experiments. 0: no enrichment. 0.05 to 5.0 µmol L^{-1}: enrichment. Box-and-whisker diagram at each nitrate concentration was compiled from the results conducted at the 8 stations. Box represents first (bottom), second (bar) and third (top) quartiles, and cross marks are the average values. Whiskers indicate minimum and maximum values, and circles are outliers. Pico: chlorophyll smaller than 2 µm (yellow). Nano: chlorophyll between 2 and 11 µm (green). Micro: chlorophyll larger than 11 µm (red). NC: naked ciliates (light blue). TC: tintinnid ciliates (light green). CN: copepod nauplii (light pink).

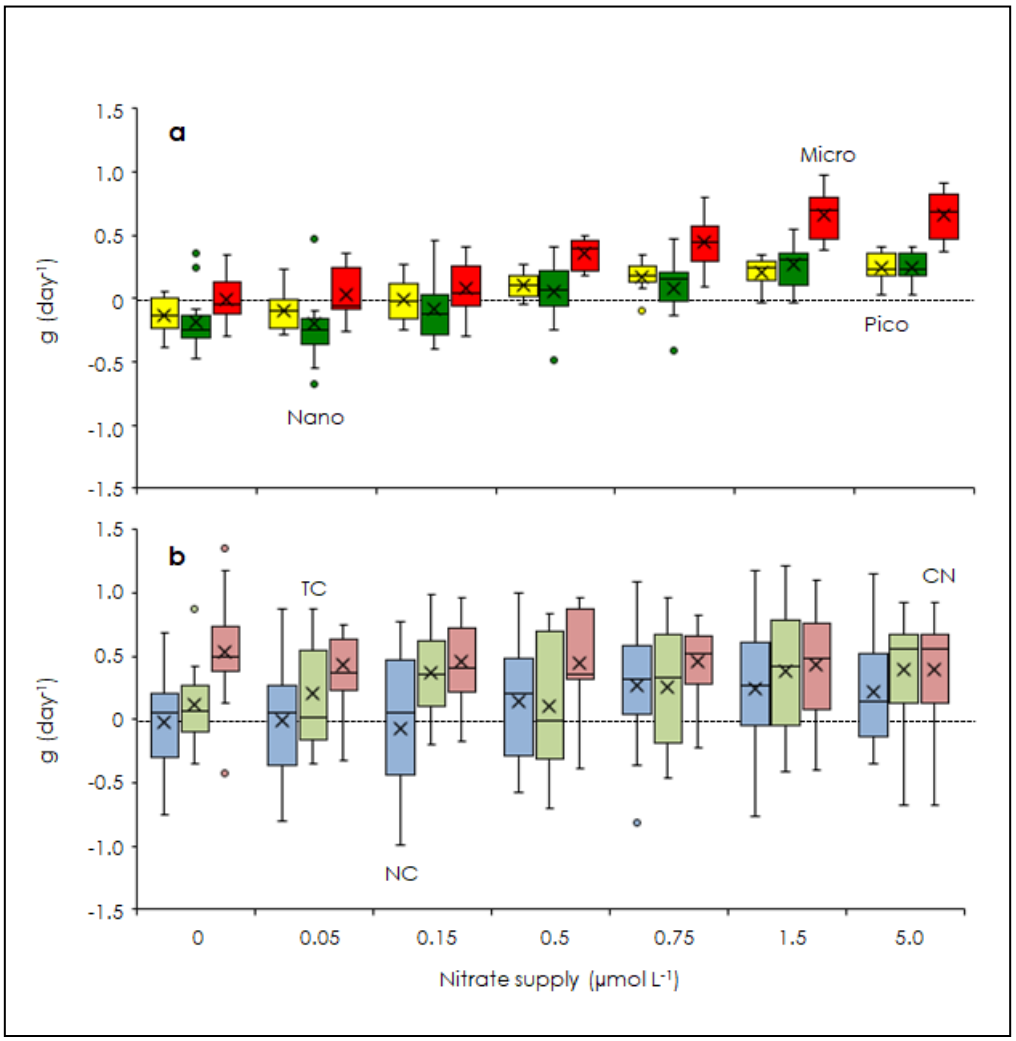

Figure 4 Changes in phytoplankton and micro-sized heterotroph growth rates in response to nitrate enrichments in the gradient enrichment experiments (EXP_a). **(a)** Growth rates (g: d^{-1}) of size-fractionated chlorophyll. **(b)** Micro-heterotroph growth rates (g: d^{-1}). 0: no enrichment. 0.05 to 5.0 µmol L^{-1}: enrichment. Box-and-whisker diagram at each nitrate concentration is based on the results conducted at the eight stations. The symbols have the same meaning as in Figure 3.

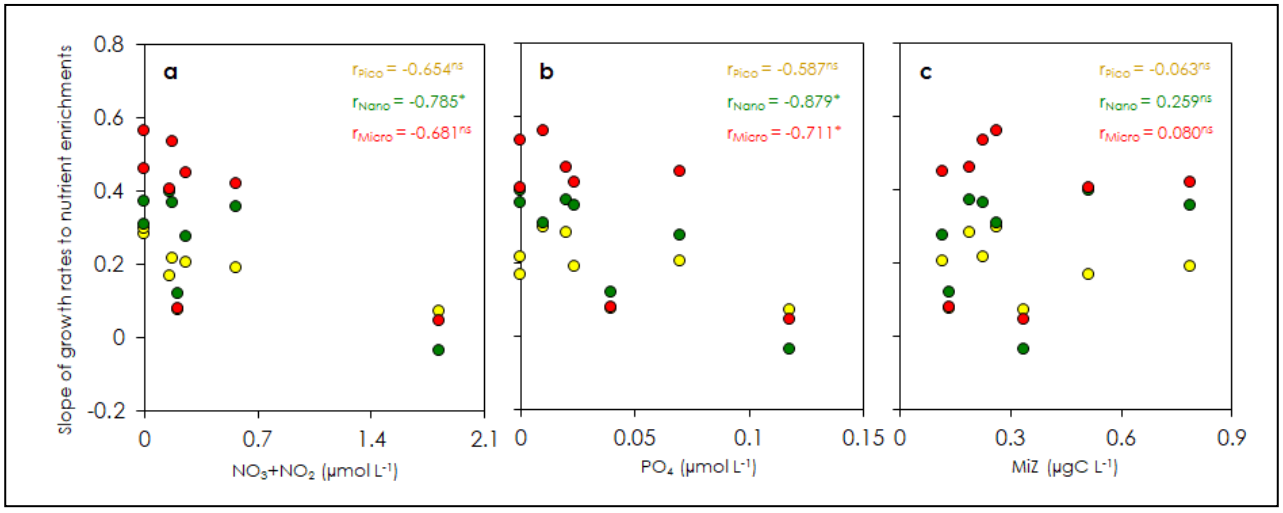

496

497 **Figure 5** Correlation of the regression slopes of phytoplankton growth rates to nutrient concentrations and micro-sized
498 heterotroph biomass at the beginning of the gradient enrichment experiments (EXP_a). **(a)** Regression slopes of the
499 size-fractionated phytoplankton growth versus the concentrations of nitrate (NO_3) plus nitrite (NO_2). **(b)** Regression
500 slopes of the size-fractionated phytoplankton growth versus the phosphate concentrations (PO_4). **(c)** Regression slopes
501 of the size-fractionated phytoplankton growth versus the micro-heterotroph biomass (MiZ). *r*: Pearson correlation
502 coefficient. Pico: chlorophyll smaller than 2 µm. Nano: chlorophyll between 2 and 11 µm. Micro: chlorophyll larger
503 than 11 µm. *: $p < 0.05$. ns: not significant.

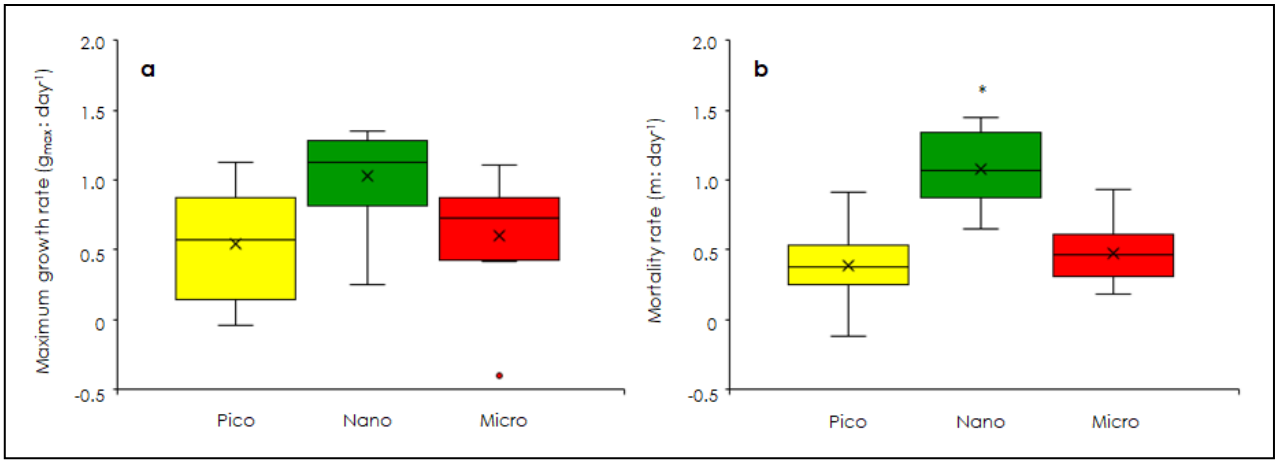

504

505 **Figure 6** Comparisons of phytoplankton growth and mortality rates among the three size-fractionated chlorophylls
506 derived from the dilution experiments (EXP_b). **(a)** Maximum growth rates (g_{max}). **(b)** Mortality rates by
507 mirozooplankton grazing. Box-and-whisker diagram at each nitrate concentration was compiled from the results
508 conducted at the 8 stations. Box represents first (bottom), second (bar) and third (top) quartiles, and cross marks are the
509 average values. Whiskers indicate minimum and maximum values, and circles are outliers. Asterisk means significant
510 difference among the three size-fractions (ANOVA + Tukey, $p < 0.05$). Pico: chlorophyll smaller than 2 µm. Nano:
511 chlorophyll between 2 and 11 µm. Micro: chlorophyll larger than 11 µm.

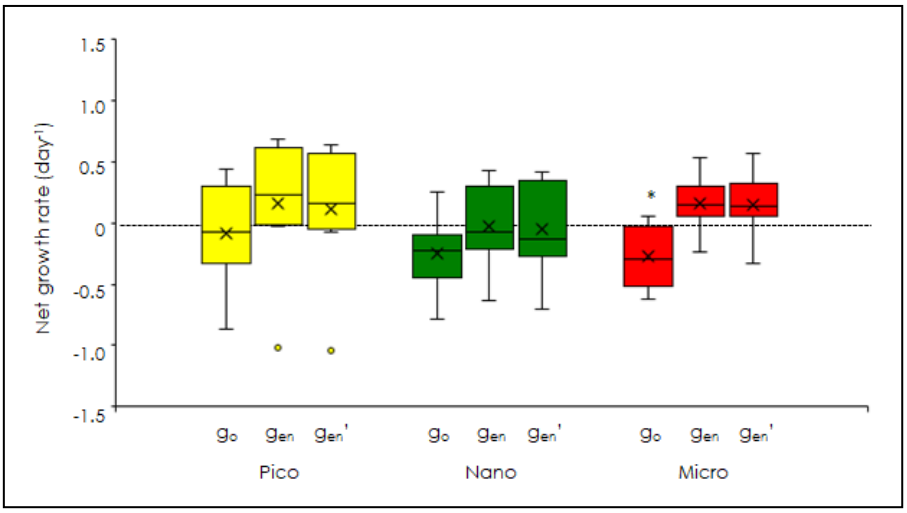

Figure 7 Comparisons of phytoplankton net growth derived from the dilution experiments (EXP_b) among the three different methods. g_o: Observed net growth rates without enrichment in the non-diluted bottles. g_{en}: Observed net growth rates with enrichment in the non-diluted bottles. g_{en}': Estimated net growth rates subtracting the mortality rates (m) from the maximum growth rates (g_{max}). Box-and-whisker diagram at each nitrate concentration was compiled from the results conducted at the 8 stations. Asterisk means significant difference between g_o and g_{en} (Welch's t-test, $p < 0.05$). The symbols have the same meaning as in Figure 6.

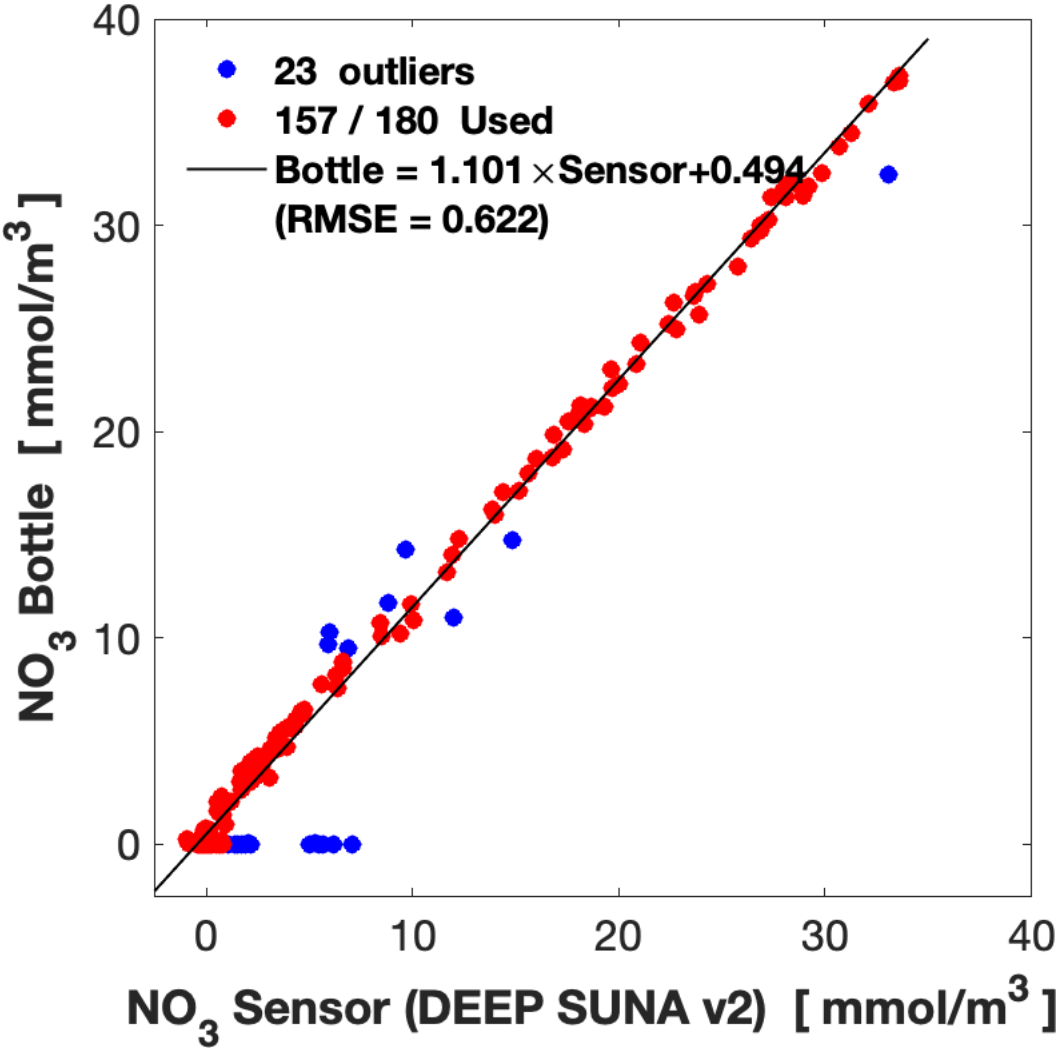

519
520

521 **Supplement Figure 1** In situ nitrate measurements by Deep SUNA V2 plotted against the laboratory water analysis
522 results from bottle sampled water during cruise KG1515 of T/S *Kagoshima-maru*. For obtaining the regression line used
523 for the sensor calibration, we excluded outlier data in which the absolute value of the difference between the data and
524 regression line exceeded 2.2 times the RMSE.

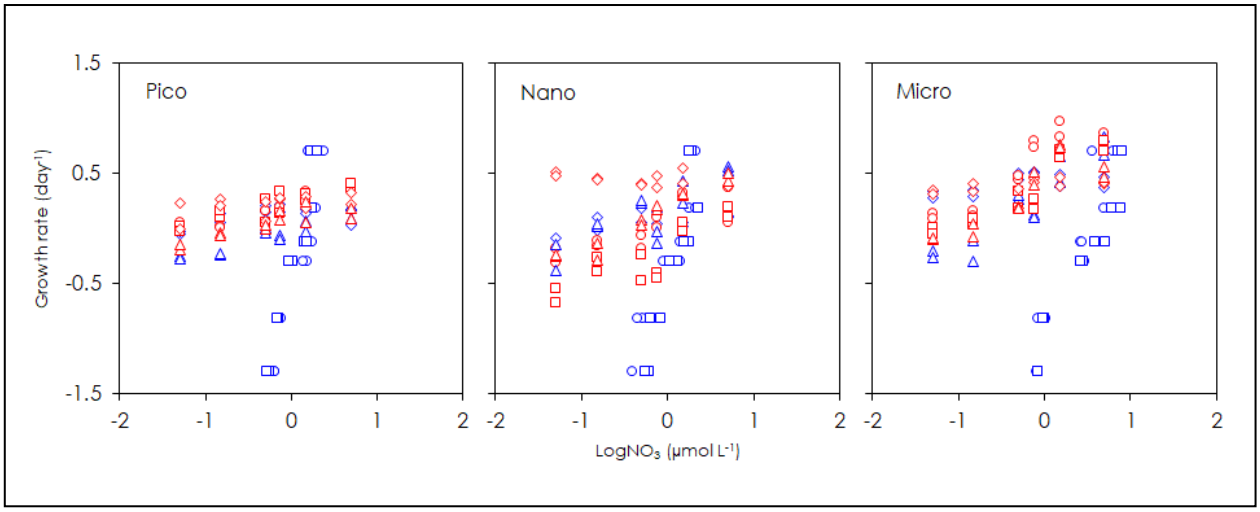

Supplement Figure 2 Relationship of phytoplankton growth rates to logarithmically transformed concentrations of enriched nitrate. Blue and red circles mean the stations in the upstream and downstream Kuroshio in the Tokara Strait, respectively. Pico: chlorophyll smaller than 2 μm. Nano: chlorophyll between 2 and 11 μm. Micro: chlorophyll larger than 11 μm.